concluded that the helicon phenomena and nonresonant cyclotron absorption can be used to make rapid and accurate measurements of the electron concentration, the effective mass, the Hall mobility, and the lattice dielectric constant. Comparison of measured values with literature values or the results of Hall and conductivity studies confirmed the validity of these techniques of experiment and analysis. We have summarized the attractive experimental regimes in the form of charts plotted in terms of the natural frequencies, ω, ω_c, ω_p, and $1/\tau$.

Although our presentation is specifically for isotropic materials with spherical constant-energy surfaces, many of these results can be generalized[32] for studying band-structure effects in anisotropic materials. In a significant group of semiconductors, however, our assumptions are well fulfilled and the analysis described above has been utilized successfully for band studies in the alloy system $Hg_{1-x}Cd_xTe$, as well as in gray tin. The techniques are applicable to a number of other semiconducting alloys and compounds. Since the techniques reported here allow the *simultaneous* measurement of N, μ, and m^*, they are very attractive for transport studies of these parameters as functions of temperature.

ACKNOWLEDGMENTS

We wish to thank Dr. G. R. Cronin of Texas Instruments Corp. for providing several InSb specimens. We also thank P. L. Radoff for his assistance with some of the experiments.

PHYSICAL REVIEW VOLUME 181, NUMBER 3 15 MAY 1969

Helicons and Nonresonant Cyclotron Absorption in Semiconductors. II. $Hg_{1-x}Cd_xTe$†‡

JOHN D. WILEY* AND R. N. DEXTER
Department of Physics, University of Wisconsin, Madison, Wisconsin 53706
(Received 25 September 1968)

We have used microwave helicons of 23 and 70 GHz and nonresonant cyclotron absorption to measure the carrier densities, effective masses, and mobilities of electrons in $Hg_{1-x}Cd_xTe$ for $0.135 \leq x \leq 0.203$. Most measurements were made at 77°K, but some values are reported for 1.3°K. Carrier concentrations at 77°K ranged from 8×10^{20} to 2×10^{22}m^{-3} and were sufficiently low to enable us to measure m^* close to the conduction-band edge. The mass values, in the range $0.004m_0$–$0.010m_0$, are in good agreement with values calculated from Kane's expression for the conduction band using literature values for the energy gap, its variation with temperature and alloy concentration, and the momentum matrix element, P. One specimen with $x=0.149$ was studied from 77 to 185°K. Over this range the mobility was closely proportional to T^{-2}. The variation of electron density permitted an estimate of the effective mass of the holes, $m_h^*=0.71m_0$.

I. INTRODUCTION

IN the preceding paper[1] (hereafter referred to as I), we described microwave techniques for making simultaneous measurements of carrier concentration N, effective mass m^*, and mobility μ in certain classes of semiconductors. These experimental techniques, helicon propagation and nonresonant cyclotron absorption (NRCA), have been used to study several samples of the alloy $Hg_{1-x}Cd_xTe$ in the neighborhood of $x=0.15$, where the Γ_6-Γ_8 energy gap goes through zero in a transition from semimetallic to semiconducting behavior. The small energy gaps at 77°K for samples with $0.08<x<0.20$ lead to extremely small electronic effective masses and strongly nonparabolic conduction bands. Due to band filling, the effective mass is a strong function of the carrier concentration. Thus, simultaneous measurements of N and m^* are ideal for studying the conduction band in $Hg_{1-x}Cd_xTe$.

It is well established[2–11] that the nonparabolicity of

† Sponsored by the Aerospace Research Laboratories, Office of Aerospace Research, U. S. Air Force.

‡ This paper is based on portions of a thesis submitted by J. D. W. in partial fulfillment of the requirements for the Ph.D. degree at the University of Wisconsin.

* Present address: Bell Telephone Laboratories, Murray Hill, N. J.

[1] John D. Wiley, P. S. Peercy, and R. N. Dexter, preceding paper, Phys. Rev. 181, 1173 (1969).

[2] T. C. Harman, A. J. Strauss, D. H. Dickey, M. S. Dresselhaus, G. B. Wright, and J. G. Mavroides, Phys. Rev. Letters 7, 403 (1961).

[3] A. J. Strauss, T. C. Harman, J. G. Mavroides, D. H. Dickey, and M. S. Dresselhaus, in *Proceedings of the International Conference on the Physics of Semiconductors, Exeter* (The Institute of Physics and the Physical Society, London, 1962), p. 703.

[4] R. Piotrzkowski, S. Porowski, Z. Dziuba, J. Ginter, W. Giriat, and L. Sosnowski, Phys. Status Solidi 8, K135 (1965).

[5] C. Verié and E. Decamps, Phys. Status Solidi 9, 797 (1965).

[6] W. Szymanska, L. Sniadower, and W. Giriat, Phys. Status Solidi 10, K11 (1965).

[7] M. Mali, Phys. Status Solidi 13, 215 (1966).

[8] W. Szymanska, Phys. Status Solidi 23, 69 (1967).

[9] W. Giriat, in *Proceedings of the International Conference on II–VI Semiconducting Compounds, Providence, 1967*, edited by D. G. Thomas (W. A. Benjamin, Inc., New York, 1968), p. 1058.

[10] R. R. Galazka and L. Sosnowski, Phys. Status Solidi 20, 113 (1967).

[11] L. Sosnowski and R. R. Galazka, in *Proceedings of the International Conference on II–VI Semiconducting Compounds, Providence, 1967*, edited by D. G. Thomas (W. A. Benjamin, Inc., New York, 1968), p. 888.

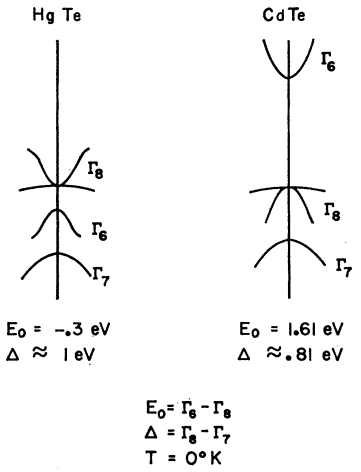

FIG. 1. Currently accepted band structures of HgTe and CdTe near $k=0$.

the HgTe and $Hg_{1-x}Cd_xTe$ conduction bands can be described by the expression obtained by Kane for InSb.[12] The work reported here confirms this for the lower portions of the conduction band. The samples used in these studies had carrier concentrations between 8×10^{20} and 2×10^{22} m^{-3} at 77°K. These relatively low N values enabled us to measure m^* near the conduction-band edge. Most previous m^* determinations for $Hg_{1-x}Cd_xTe$ with $0\leq x\leq0.3$ have been performed on samples with much higher carrier concentrations.[4–11] A few mass values have been reported for samples with low N values[2,3] but they are quite limited in number and the masses and carrier concentrations were determined in separate experiments. In order to perform a systematic test of the applicability of Kane's theory and to obtain an accurate determination of the momentum matrix element P, one should ideally have several samples with different carrier concentrations for each x value. This would allow measurements of m^* as a function of N at a given, fixed temperature T. Otherwise N must be varied by changing T, and one must include in the analysis the temperature dependence of the energy gap. Any uncertainty in $E_g(T)$ then clouds the P determination. Since we were unable to obtain the necessary sets of samples, no such systematic test of Kane's model was attempted. Rather, we have measured m^* for each of seven samples with x values between 0.135 and 0.203 at 77°K, and for a few samples at other temperatures as well. The measured masses are then compared with values calculated using Kane's theory together with E_g, dE_g/dT, and P values taken from the published literature. In Sec. II of this paper, we discuss the $Hg_{1-x}Cd_xTe$ alloy system, Kane's model for the conduction band, and our choices for the parameters needed in this model. Section III contains our experimental observations, including a brief discussion of the temperature dependence of N and μ for one sample. Section IV summarizes our results and conclusions.

[12] E. O. Kane, J. Phys. Chem. Solids **1**, 249 (1957).
[13] W. D. Lawson, S. Nielsen, E. H. Putley, and A. S. Young, J. Phys. Chem. Solids **9**, 325 (1959).

II. HgTe-CdTe ALLOY SYSTEM

A. Energy-Gap Parameters

The compounds HgTe and CdTe have been shown[13] to be mutually soluble in all proportions, forming a single-phase disordered alloy $Hg_{1-x}Cd_xTe$ over the entire range of x from 0 to 1. Since the endpoint materials both crystallize in the zinc-blende structure and have very similar lattice constants (6.462 Å for HgTe and 6.482 Å for CdTe),[14] one expects the physical properties of the alloys to vary smoothly with x. It has now been experimentally verified[15] that many physical parameters, in fact, vary *linearly* with x. Both HgTe and CdTe have received considerable attention in recent years and their band structures are thought to be those shown in Fig. 1. The HgTe band structure[16] is similar to that proposed by Groves and Paul[17] for gray tin, and it is this fact which gives the $Hg_{1-x}Cd_xTe$ system some of its most interesting and unusual properties. Figure 2 depicts the band structure of $Hg_{1-x}Cd_xTe$ in the neighborhood of $x=0.15$. It is in this region that the system undergoes a transition from the semimetallic structure of HgTe to a semiconducting band structure with a positive energy gap. Both the linear dependence of E_g on x and the strong interaction of the conduction and light hole bands shown in Fig. 2 are well confirmed experimentally.[15,18]

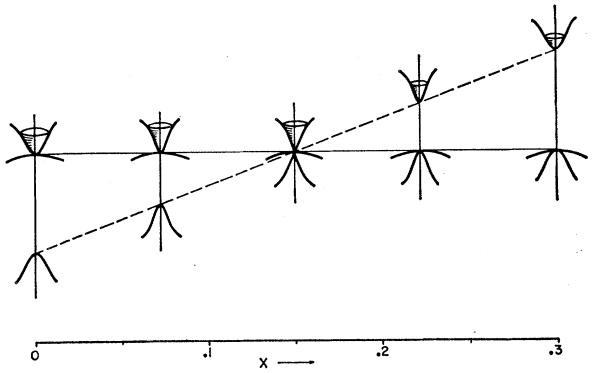

FIG. 2. Schematic representation of the band structure of $Hg_{1-x}Cd_xTe$ near $x=0.15$. The shading in the conduction band is meant to depict the band filling caused by the extreme disparity between the electron and hole effective masses.

[14] J. C. Wooley and B. Ray, J. Phys. Chem. Solids **13**, 151 (1960).
[15] D. Long, Honeywell Corporate Research Center Final Contract Report, 1966 (unpublished).
[16] T. C. Harman, W. H. Kleiner, A. J. Strauss, G. B. Wright, J. G. Mavroides, J. M. Honig, and D. H. Dickey, Solid State Commun. **2**, 305 (1964).
[17] S. H. Groves and W. Paul, Phys. Rev. Letters **11**, 505 (1963); in *Proceedings of the Seventh International Conference of the Physics of Semiconductors, Paris, 1964* (Dunod Cie., Paris, 1964), p. 41.
[18] C. Verié, Phys. Status Solidi **17**, 889 (1966).

In the early literature on $Hg_{1-x}Cd_xTe$, there was some uncertainty as to whether the Γ_6-Γ_8 energy gap E_g varied linearly with x or with the lattice parameter a_0.[16,19] Since that time, however, a considerable amount of experimental evidence has been published in support of the linear variation of E_g with x.[9,11,15,20–23] The variation of E_g with temperature is also a matter on which there is some disagreement in the literature. There are a few well established determinations, however, and these lend weight to our assumed linear variation of dE_g/dT with x. From a compilation of the results of measurements of E_g for HgTe at temperatures between 1.5 and 300°K [5,18,24,25] one can infer a linear change of E_g with T of $dE_g/dT=+5\times10^{-4}$ eV/°K, with E_g ranging from -0.303 eV at 1.5°K to -0.15 eV at 300°K. Groves[26] has suggested a slight deviation from linearity at the lowest temperatures, but this will not be important for the present work. The CdTe band gap varies from 1.606 eV at 1.6°K [27] to $\sim$1.45 eV at 300°K,[28] giving an approximate rate of $dE_g/dT=-5\times10^{-4}$ eV/°K. The assumption of a linear temperature dependence is less well satisfied for CdTe than for HgTe (dE_g/dT is somewhat larger than the above number at high temperatures and smaller at low temperatures), but since we will be concerned with the Hg-rich end of the alloy system, this is an unimportant detail.

The fact that the dE_g/dT values for HgTe and CdTe are approximately equal in magnitude and opposite in sign, together with the linear dependence of E_g on x, implies that $dE_g/dT\approx0$ for $x\approx0.5$. This has been experimentally verified[15] and lends further weight to the above assumptions. Several other measured values of dE_g/dT also lie on a linear extrapolation between the endpoint values.[23,29] Thus, we are led to adopt the following expression for the energy gap of $Hg_{1-x}Cd_xTe$ as a function of temperature and x:

$$E_g(x,T)=-0.30+5\times10^{-4}T+(1.91-10^{-3}T)x. \quad (1)$$

If this is solved for the x value which gives $E_g=0$ (the semimetal-semiconductor transition), one obtains

$$x_0=(0.30-5\times10^{-4}T)/(1.91-10^{-3}T). \quad (2)$$

This gives $x_0=0.157$ at 0°K, $x_0=0.143$ at 77°K, and $x_0=0.093$ at 300°K. These numbers are in excellent agreement with several authors,[9–11,15] particularly at the lower temperatures, but differ slightly with others[22] primarily due to different choices of dE_g/dT for HgTe.

The other parameter needed to describe the nonparabolicity of the $Hg_{1-x}Cd_xTe$ conduction band is the momentum matrix element P. This parameter is more conveniently expressed as an energy $E_P=(2m_0/\hbar^2)P^2$, where m_0 is the free electron mass. If one accepts the values $E_P=18\pm1$ eV for HgTe[24] and 21 eV for CdTe [30] and assumes no temperature dependence and linear x dependence, one obtains

$$E_P=(18+3x) \text{ eV}. \quad (3)$$

The temperature independence and linear x dependence seem well confirmed experimentally,[11] but different numbers have sometimes been used for E_P(CdTe).[11] Our limited number of samples and their narrow range of x values prevent confirmation of the slight x dependence of E_P. Equation (3) will be used in the analysis because it is more realistic than assuming a constant E_P value.

B. Conduction-Band Effective Mass

As mentioned in the Introduction, the conduction band of $Hg_{1-x}Cd_xTe$ is thought to be well described by the expression derived by Kane for InSb.[12] There are many adequate discussions of Kane's method[12,31,32] and its application to $Hg_{1-x}Cd_xTe$.[2–11,24,32,33] The result needed for the present discussion is the following. Assuming that the spin-orbit interaction energy $\Delta=E(\Gamma_8)-E(\Gamma_7)$ is $\gg|E_g|$, kP and neglecting any interactions with higher bands, the shape of the conduction band near $k=0$ is given by

$$E_c=\hbar^2k^2/2m_0+\tfrac{1}{2}[|E_g|+(|E_g|^2+\tfrac{4}{3}P^2k^2)^{1/2}], \quad (4)$$

where k is the wave vector of the electron, P is the momentum matrix element, and the energy is measured relative to the bottom of the conduction band. The assumption of large Δ is well satisfied for the work reported here since $\Delta\approx1$ eV [24] and, for our samples, $|E_g|$ and kP are both $\lesssim0.1$ eV. Furthermore, it has been noted[24] that the errors, introduced by assuming $\Delta\to\infty$ and by neglecting higher bands, tend to cancel. Using

[19] M. D. Blue, Phys. Rev. **134**, A226 (1964).
[20] Rudolf Ludeke and William Paul, J. Appl. Phys. **37**, 3499 (1966).
[21] T. C. Harman, in *Proceedings of the International Conference on II-VI Semiconducting Compounds, Providence, 1967*, edited by D. G. Thomas (W. A. Benjamin, Inc., New York, 1968), p. 982.
[22] C. Verié, in *Proceedings of the 1967 International Conference on the Physics of II-VI Semiconductors, Providence, 1967*, edited by D. G. Thomas (W. A. Benjamin, Inc., New York, 1968), p. 1124.
[23] Warren Saur (private communication).
[24] S. H. Groves, R. N. Brown, and C. R. Pidgeon, Phys. Rev. **161**, 779 (1967).
[25] C. R. Pidgeon and S. H. Groves, in *Proceedings of the International Conference on II–VI Semiconducting Compounds, Providence, 1967*, edited by D. G. Thomas (W. A. Benjamin, Inc., New York, 1968), p. 1080.
[26] S. H. Groves, Bull. Am. Phys. Soc. **12**, 1031 (1967).
[27] D. G. Thomas, J. Appl. Phys. Suppl. **32**, 2298 (1961).
[28] This does not correspond to a single measured value but is an average of many published numbers ranging from 1.39 to 1.50 eV. See, for example, D. de Nobel, Philips Res. Rept. **14**, 361 (1959); E. Konak, Phys. Status Solidi **3**, 1274 (1963).
[29] C. Verié and R. Granger, Compt. Rend. **261**, 3349 (1965).
[30] M. Cardona, J. Phys. Chem. Solids **24**, 1543 (1963).
[31] E. O. Kane, in *Semiconductors and Semimetals*, edited by R. K. Willardson and A. C. Beer (Academic Press Inc., New York, 1966), pp. 75–100.
[32] D. Long, *Energy Bands in Semiconductors* (Wiley-Interscience, Inc., New York, 1968).
[33] W. Gorzkowski, Phys. Status Solidi **11**, K131 (1965); **15**, K9 (1966).

the expression for the cyclotron mass,

$$\frac{m^*}{m_0}=\frac{\hbar^2}{m_0}\left(\frac{1}{k}\frac{dE}{dk}\right)^{-1}, \tag{5}$$

together with Eq. (4), one obtains for the effective mass

$$\frac{m^*}{m_0}=\left[1+\frac{4P^2m_0}{3\hbar^2}\left(|E_g|^2+\frac{8P^2k^2}{3}\right)^{-1/2}\right]^{-1}, \tag{6}$$

or, in terms of E_P,

$$\frac{m^*}{m_0}=\left[1+\frac{2}{3}\left(\left|\frac{E_g}{E_P}\right|^2+\frac{4\hbar^2k^2}{3m_0E_P}\right)^{-1/2}\right]^{-1}. \tag{7}$$

At $k=0$ one obtains the conduction-band-edge mass m_n^*/m_0 given by

$$m_n^*/m_0=(1+\tfrac{2}{3}|E_P/E_g|)^{-1}. \tag{8}$$

This is frequently written in the approximate form $m_n^*/m_0\approx 3|E_g|/2E_P$. From the expressions for m^* and m_n^* it is seen that the effective mass of electrons

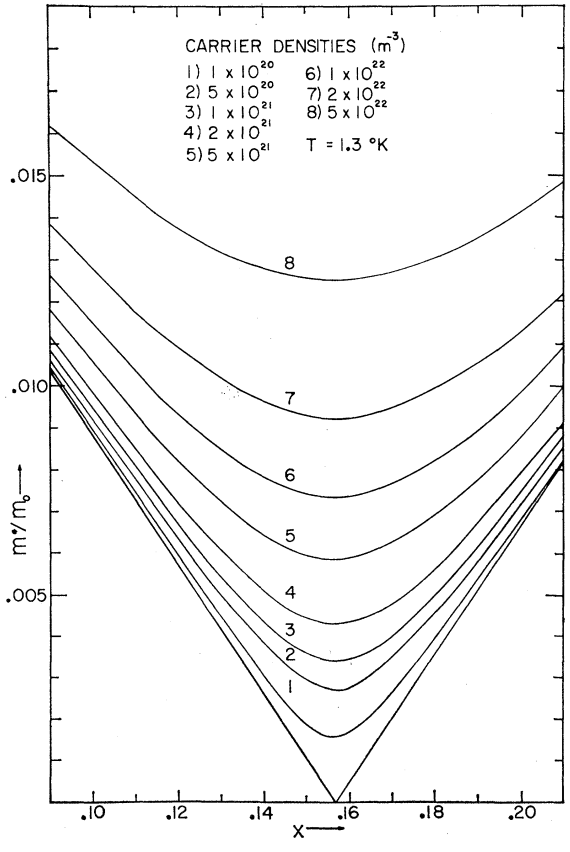

FIG. 3. Conduction-band effective mass as a function of x at 1.3°K for various assumed carrier concentrations. Note that the sharp dependence of m^* on x is substantially washed out at higher carrier densities.

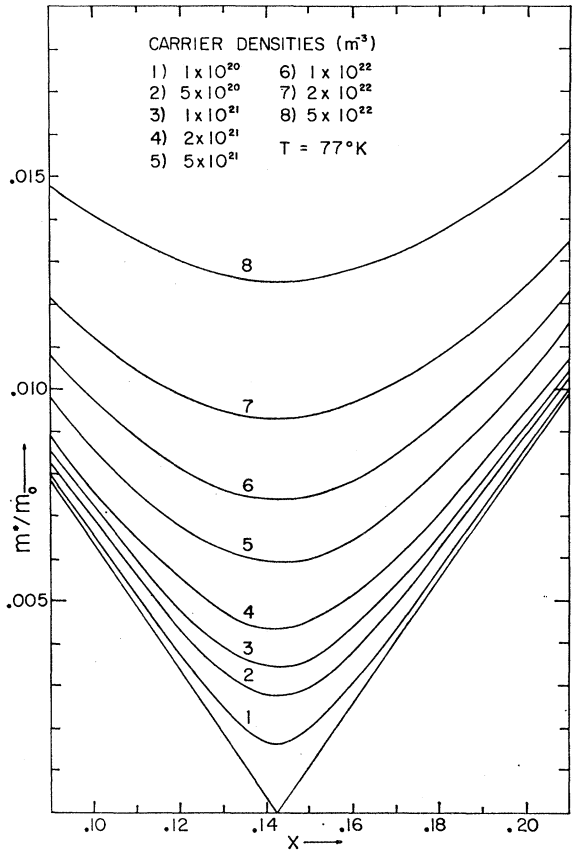

FIG. 4. Conduction-band effective mass as a function of x at 77°K for various assumed carrier concentrations.

near the conduction-band edge in $Hg_{1-x}Cd_xTe$ should be extremely small for x values near the point where $E_g=0$. In order to observe these small masses, however, the carrier densities must be rather low. Due to the high density of states in the valence band, the Fermi level is pushed well up into the conduction band even at moderately low carrier densities. If we assume a spherical Fermi surface and a degenerate electron gas in the conduction band, we can write

$$k_F^2=(3\pi^2N)^{2/3}, \tag{9}$$

where k_F is the value of k at the Fermi surface and N is the electron density. Using Eqs. (1), (3), (7), and (9), we have evaluated m^* as a function of x and N at various temperatures. The results are shown in Figs. 3 and 4 for $T=1.3$ and 77°K, respectively. As noted earlier, the x dependence of E_P is not strong enough to be noticeable over so small a range of x values. Thus, the deviation of the band-edge mass from linearity is scarcely perceptible in Figs. 3 and 4. Qualitatively, the mass curves are simply translated rigidly to lower x values as T increases [nonlinearly but roughly at the rate 2.2×10^{-4} (mole fraction)/°K]. This is not, of course, a correct quantitative description of the tempera-

ture dependence of these curves, but it may be used to obtain m^* values for temperatures between 1.3 and 77°K or above. The simplest procedure is to use Eq. (2) to calculate the expected position of x_0 and then translate the x scale, accordingly. The error introduced by ignoring slight changes in the shapes of these curves will be least near x_0.

III. EXPERIMENTAL

A. Samples

Our samples were generously provided by Schmit and Long of the Honeywell Corporate Research Center and Strauss of the Lincoln Laboratory, MIT. Most of them were polycrystalline, consisting of 2–3 large crystallites. They could always be mounted in such a way that the microwaves passed through only a single crystallite, however, and no special effects were noted in cases where the microwaves were allowed to pass through parts of adjacent crystallites simultaneously. The x values of the samples which we obtained from Honeywell had been determined by them, using density measurements. These numbers were confirmed by us to ±5% accuracy using electron microprobe techniques. The numbers which we quote for these samples are those obtained by the density techniques, since they are expected to be more accurate.[34,35] It should also be pointed out that the density measurements yield an average x value for the entire sample, whereas microprobe measurements are performed on small chips removed from the edges of the samples. Both average and local x values could be misleading if there were appreciable sample nonuniformity. The x values which we quote for the samples obtained from the Lincoln Laboratory (samples A and B) are based solely on our own microprobe measurements.

It is important in these experiments that the samples be homogeneous in x and N. Inhomogeneities tend to smear out the interference structure and can lead to changes in the interference condition similar to those discussed in connection with Eq. (13) of I. Of the 11 samples which we obtained, seven were completely satisfactory for our studies. We have seen nothing in visual microscopic inspections, microprobe studies of small chips, or in the experimental data which would indicate that these seven samples are inhomogeneous in composition. Any gradients in N were sufficiently small to be of no important consequence. The most extreme case involved a variation from 1.7×10^{22} to 2.2×10^{22} m^{-3} over a distance of 7 mm, and in most cases there was no N variation within our experimental accuracy. Of the remaining four samples, two showed no interference structure at all and two showed faint fringes with beating patterns, which indicated that the waves were travelling along multiple paths of different average index of refraction. On close inspection, the latter two samples were observed to have numerous tiny fissures and pockets of free Hg. More of these were revealed upon further lapping of these samples. Furthermore, we have recently learned[34] that at least one and possibly both of the samples which showed no interference structure were taken from regions of the original boules which were characterized by steep x gradients.

Sample preparation and mounting presented no particular difficulties. The samples were lapped to the desired thickness and then given a light etch in a solution of 15–20% (by volume) Br in methanol. The resulting slabs ranged in thickness from 0.59 to 1.65 mm and had lateral dimensions sufficiently large to make it unnecessary to apply geometric corrections. [See the discussion associated with Eq. (4) in I.] The samples were held over the coupling iris of the microwave cavity by two or three small dots of Flexrock Adhesive No. 80 (Flexrock Co., Phila.) or by small mounting clips, which pressed lightly against the extreme edges of the back side of the sample.

B. Observations

Most of our experiments were performed at 77°K using circularly polarized 24- and 70-GHz microwaves. Some typical experimental traces are shown in Figs. 5–7. The traces were taken using magnetic field modulation and synchronous detection at 500 cps. The y axis was driven by the output of the phase-sensitive detector (Princeton Applied Research lock-in amplifier model HR-8) and is proportional to the field derivative of the reflected microwave signal. The x axis was driven by a Hall probe, which monitored the applied dc magnetic field. The microwave system was described in I and will not be further discussed here.

Figure 5 shows a trace taken at 77°K and 70 GHz for sample 4. This sample had both low carrier density

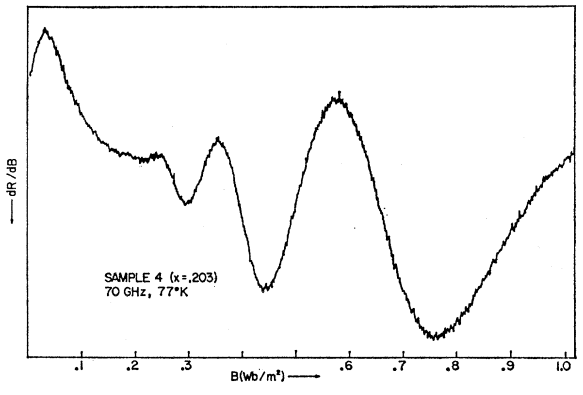

FIG. 5. Experimental trace taken for sample 4 at 70.7 GHz and 77°K. The interference fringes are due to dimensional or Fabry-Perot resonances, which occur as a consequence of the magnetic field dependence of the conduction-electron contribution to the index of refraction. Sample 4 had a low carrier concentration and hence produced only a few interference fringes. The sample thickness was 1.03 mm.

[34] Dr. J. Schmit (private communication).
[35] R. R. Galazka, Acta Phys. Polon. 24, 791 (1963).

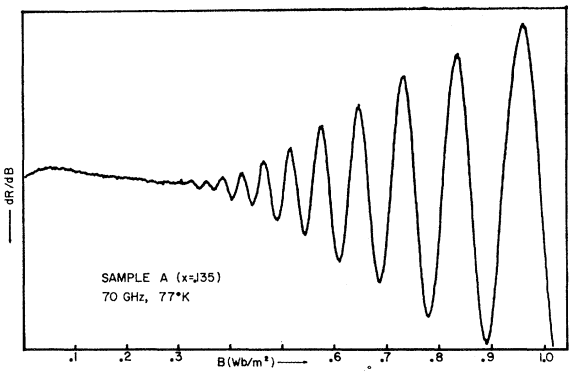

FIG. 6. Experimental trace taken for sample A at 70.6 GHz and 77°K. The sample thickness was 1.06 mm. The microwaves were linearly polarized for this case.

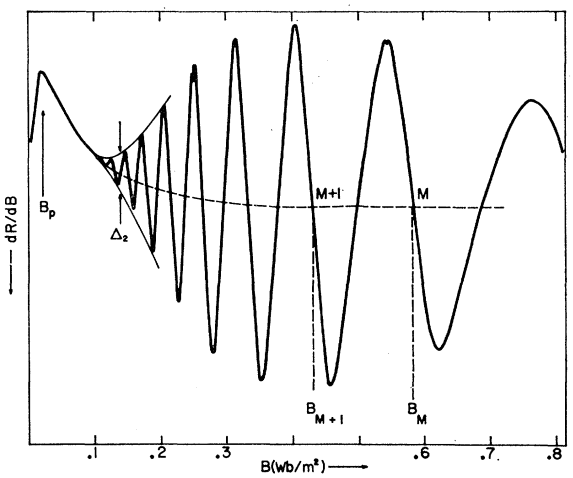

FIG. 8. Experimental curve which illustrates the sources of our experimental data. The low-field peak B_p, the opening part of the amplitude envelope Δ_2, and the field positions of the interference fringes B_M, contain useful and partially redundant information about N, m^*, μ, and ϵ_L. This trace was taken for sample E at 23.7 GHz and 77°K. The sample thickness was 0.88 mm.

and relatively low mobility. Thus, we were able to observe only a small number of interference fringes. This trace is typical of the *lowest* quality data which were analyzed. Figure 6 shows a trace taken for sample A at 77°K and 70 GHz. The large number of closely spaced fringes indicates that this sample has a higher carrier density than sample 4. An analysis of the amplitude envelope indicates that the mobility is higher, as well. Figure 7 shows data for sample I at 24 GHz and 77°K. The recorder pen was lifted and immobilized briefly at ~ 0.8 Wb/m^2 while the field swept through a sharp spin-resonance line, which is sometimes used for field calibration. The interference structure at extremely low fields and the sharp low-field peak at B_P (See Sec. II B of I) are characteristic of a high-mobility sample.

The theoretical expressions needed to analyze our data were discussed in I. The main results are contained in the following expressions:

$$M^2=\left(\frac{\omega L}{\pi C}\right)^2\frac{\epsilon_L}{\epsilon_0}+\left(\frac{\omega L}{\pi C}\right)^2\frac{Ne}{\epsilon_0\omega B_M}\left(1+\frac{B_r}{B_M}\right), \quad (10)$$

$$\ln(\Delta_2 B^{1/2})=C_3-C_2B^{-3/2}, \quad (11)$$

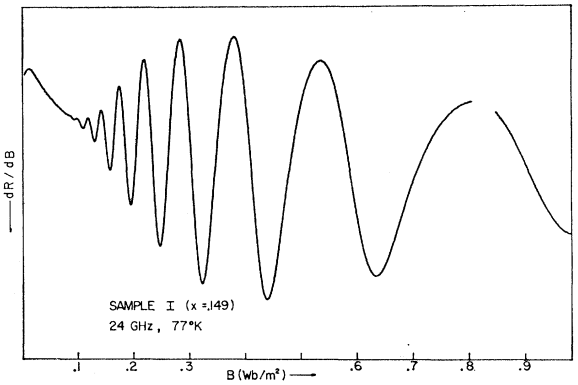

FIG. 7. Photograph of an experimental trace taken for sample I at 23.7 GHz and 77°K. The sample thickness was 0.83 mm.

and

$$B_P=B_r+K/\mu, \quad (12)$$

where the observed quantities required in these expressions are obtained from experimental traces in the manner illustrated in Fig. 8. Definitions of the remaining symbols are to be found in I.

Figure 9 shows a plot of M^2 versus $1/B_M$ and also versus $1/B_M+B_r/B_M^2$ with $B_r=0.004$ Wb/m^2 (corresponding to $m^*=0.0048m_0$). This plot is based on data taken at 23 GHz and 1.3°K for sample I. The effect of the B_r/B_M^2 term is clearly evident in the nonlinearity of the M^2 versus $1/B_M$ plot. From Eq. (10), it is seen that the slope of the straight line gives N, the B_r

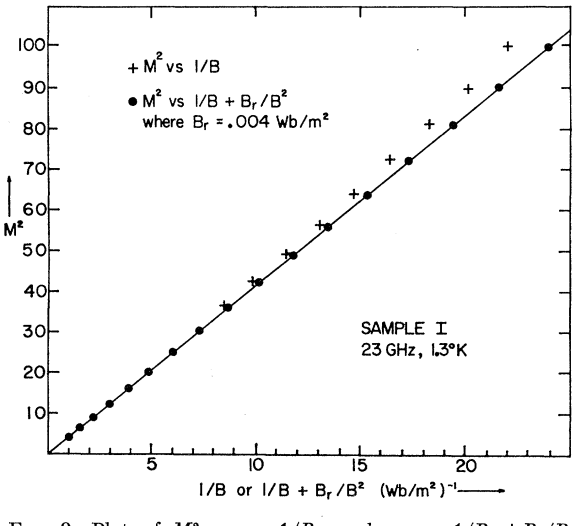

FIG. 9. Plot of M^2 versus $1/B_M$ and versus $1/B_M+B_r/B_M$ using data taken for sample I at 23 GHz and 1.3°K. The B_r value used corresponds to $m^*/m_0=0.0048$. This plot is based on Eq. (10).

TABLE I. Values of the carrier density N and mobility μ measured at K (24 GHz) and V (70 GHz) bands and 77°K for each of our samples of $Hg_{1-x}Cd_xTe$. Effective-mass values measured at V band by helicon analysis are compared with theoretical values of the effective mass computed for the Kane model using literature values of energy-gap parameters.

Sample	x	N_K (m^{-3})	N_V (m^{-3})	μ_K (m^2/V sec)	μ_V (m^2/V sec)	$(m_V^*/m_0)_{\text{expt}}$	$(m^*/m_0)_{\text{theor}}$
A	0.135	1.7×10^{22}	1.7×10^{22}	38±2	36±3	0.010 ±0.0015	0.0090
E	0.144	7.9×10^{21}	8.0×10^{21}	56±3	61±4	0.0068±0.0005	0.0068
I	0.149	6.8×10^{21}	6.7×10^{21}	64±4	58±5	0.0069±0.0004	0.0066
B	0.150	2.3×10^{22}	2.3×10^{22}	38±3	31±3	0.010 ±0.002	0.0098
7	0.188	1.4×10^{21}	1.4×10^{21}	24±1	23±1	0.0076±0.0005	0.0078
J	0.193	3.4×10^{21}	3.5×10^{21}	28±2	26±2	0.0085±0.0015	0.0091
4	0.203	9.0×10^{20}	8.9×10^{20}	19±1	18±2	0.010 ±0.003	0.0094

correction needed to achieve linearity gives m^*, and the intercept gives ϵ_L. In all of our samples, even at 1.3°K, the carrier densities were too large to permit accurate measurements of ϵ_L. Our data are consistent, however, with values of ϵ_L/ϵ_0 between 18 and 19. This is what would be expected from a linear interpolation between the endpoint values[15] of 20 for HgTe and 10 for CdTe. The amplitude analysis is illustrated in Fig. 10, where we show a plot of $\ln\Delta_2 B^{1/2}$ versus $B^{-3/2}$. This plot is based on data taken at 24 GHz and 77°K for sample I. The slope of the line in Fig. 10 is proportional to $-\mu^{-1}$.

All of our samples had sufficiently high $\omega\tau$ values at 70 GHz and 77°K to allow m^* determinations from helicon interferometry at that frequency. (See the discussion associated with Fig. 1 of I. The above statement implies that the samples were all in the B region of Fig. 1 at 70 GHz.) As pointed out in I, these m^* values are more reliable than those determined from the inflection point or NRCA techniques. For this reason, the m^* values determined by the latter techniques will not be emphasized. In all cases where careful B_P analyses were performed, the resulting m^* values were within 20% of the values determined from helicon analysis.

The N, μ, and m^* values determined from helicon interferometry at 77°K are collected in Table I. The subscripts K and V refer to K-band (~24 GHz) and V-band (~70 GHz) microwaves. The theoretical m^* given in the last column was calculated using Eqs. (1), (3), (7), and (9) together with the experimental N values. In Table II we present the results of similar experiments performed at 1.3°K. At this temperature $\omega\tau$ was large enough at 23 GHz to allow m^* determinations from helicon analysis. All the results in Table II are based on experiments at this frequency. In order to display graphically the extent to which band filling has occurred in these samples, the 77°K m^* values are plotted in Fig. 11 on a diagram similar to Fig. 4. Where available, m^* values determined by the NRCA techniques [Eq. (12)] are also included in Fig. 11 for comparison.

TABLE II. Values of the carrier density N and electronic effective mass measured at 23 GHz and 1.3°K by means of helicon analysis for several samples of $Hg_{1-x}Cd_xTe$. Measured effective masses are compared with theoretical values computed according to Kane's model using literature values of energy-gap parameters.

Sample	x	N_K (10^{21} m^{-3})	$(m_K^*/m_0)_{\text{expt}}$	$(m^*/m_0)_{\text{theor}}$
E	0.144	2.0	0.0055±0.0015	0.0047
I	0.149	2.0	0.0048±0.0007	0.0045
B	0.150	1.31	0.0075±0.0015	0.0082
7	0.188	1.14	0.0067±0.0010	0.0059

When discussing the N dependence of m^*, it is customary to note that Eq. (7) can be written as

$$\left(\frac{m_r^*}{1-m_r^*}\right)^2=\left(\frac{3\hbar^2}{4m_0}\right)^2\frac{E_g^2}{P^4}+\left(\frac{3\hbar^2}{4m_0}\right)^2\frac{8(3\pi^2)^{2/3}}{3P^2}N^{2/3}, \quad (13)$$

where $m_r^*=m^*/m_0$. Thus, for a series of samples with a given E_g, a plot of $[m_r^*/(1-m_r^*)]^2$ versus $N^{2/3}$ should give a straight line whose slope and intercept determine P and E_g. If one uses samples with different E_g's (different x values) or varies N by varying T, however, $E_g(x,T)$ must be known in advance and the plot of $[m_r^*/(1-m_r^*)]^2$ versus $N^{2/3}$ is no longer linear. In such cases Eq. (13) is more useful if written as

$$\left(\frac{m_r^*}{1-m_r^*}\right)^2N^{-2/3}=\left(\frac{3\hbar^2}{4m_0}\right)^2\frac{E_g^2N^{-2/3}}{P^4}+\left(\frac{3\hbar^2}{4m_0}\right)^2\frac{8(3\pi^2)^{2/3}}{3P^2}. \quad (14)$$

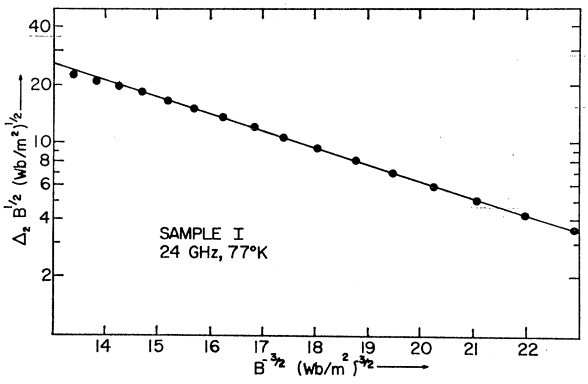

FIG. 10. Plot of $\ln\Delta_2 B^{1/2}$ versus $B^{-3/2}$ based on data taken for sample I at 24 GHz and 77°K. The slope of this line is $\propto -\mu^{-1}$. The points on the linear portion were taken between 0.10 and 0.17 Wb/m^2 from a trace similar to that shown in Fig. 7.

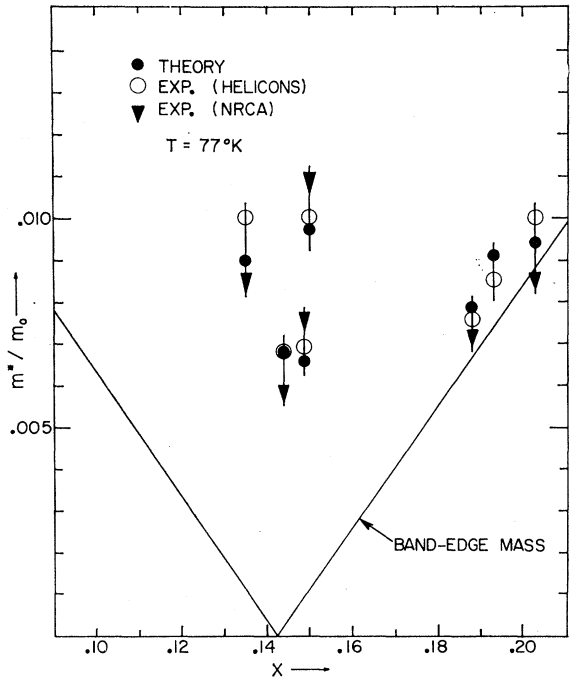

FIG. 11. Experimental and theoretical m^* values shown on a diagram similar to Fig. 4 in order to show the extent to which band filling has taken place for each of our samples at 77°K.

One now plots $[m_r^*/(1-m_r^*)]^2N^{-2/3}$ versus $E_g^2N^{-2/3}$ to obtain a straight line and possibly a determination of P. Figure 12 shows this type of plot for our 77 and 1.3°K results from Tables I and II on the assumption that P is independent of temperature.[10] The four lines correspond to $E_P=17$, 18, 19, and 20 eV. The values of E_P used elsewhere in this paper were based on Eq. (3) (~18.3 eV). From Fig. 12 it is clear that, while the data are adequately described by the E_P of Eq. (3),

TABLE III. Values of the carrier density N, mobility μ, and effective mass m^*, measured at several temperatures for sample I, $x=0.149$. The measured values of effective mass are compared with mass values computed according to Kane's model, using literature values of energy-gap parameters. The N and m^* values were obtained from helicon interferometry at 70 GHz and the μ values from amplitude analysis at 24 GHz.

T (°K)	N (m^{-3})	μ (m^2/V sec)	$(m^*/m_0)_{expt}$	$(m^*/m_0)_{theor}$
1.3	2.0×10^{21}	180±30	0.0048±0.0006	0.0044
77	6.8×10^{21}	64±4	0.0069±0.0004	0.0065
87	8.3×10^{21}	47±4	0.0073±0.0006	0.0070
100	1.0×10^{22}	38±3	0.0070±0.0008	0.0075
125	1.5×10^{22}	26±2	0.0082±0.0010	0.0082

other values might do as well under slightly different assumptions for $E_g(x,T)$.

C. Temperature Dependence of N, μ, and m^*

Sample I, with $x=0.149\pm0.002$, was investigated at 1.3°K and from 77–185°K at both 23 and 70 GHz in a study of the temperature dependence of N, μ, and m^*. Sample I was chosen for this study for several reasons. Of our samples near the zero-gap concentration, this sample had the lowest carrier density and gave the best hope of observing intrinsic behavior in the temperature range available. It also had the highest 77°K mobility and hence allowed us to obtain m^* values at higher temperatures than would have been possible with other samples. It was hoped that a study of N versus T would provide an estimate of the effective mass of the holes and that by measuring μ versus T, we could make some statement on the pertinent scattering mechanisms. These goals were only partially realized. In Table III, we present data on N, μ, and m^* versus T for a few chosen temperatures at which full m^* analyses were performed. The theoretical m^* values which are included for comparison were calculated in the manner

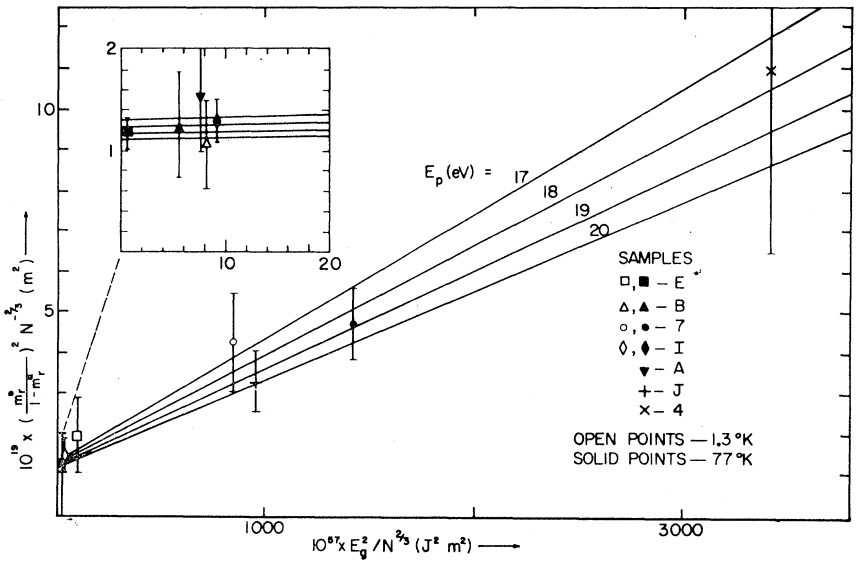

FIG. 12. Plot based on Eq. (14) which shows that an E_P value between 18 and 19 gives the best fit to our data for the $E_g(x,T)$ expression used.

described in Sec. II B. The limited data on variation of m^* with N and T at constant x are clearly consistent with the Kane model and with the assumed $E_P(x)$ and $E_g(x,T)$ discussed in Secs. II B and III B.

The mobility was measured by helicon amplitude analysis over the range 77–185°K, where it varies approximately as $T^{-2.0}$, as shown in Fig. 13. This result is in accord with some other mobility measurements in similar crystals.[15] Verié[18] has made a more complete study of the temperature variation of the mobility. He has concluded that the dominant mechanism at higher temperatures is acoustic-phonon scattering of electrons. On the other hand, Galazka and Sosnowski[10] describe the variation of mobility with temperature (77–300°K) by combined optical-mode and ionized-impurity scattering for a specimen with $x=0.10$. Our specimen undergoes a relatively large change in the energy gap and effective mass over the temperature range investigated. As a consequence, we merely quote our result; no further analysis seems appropriate for such limited data.

From a study of the temperature dependence of N over the range 77–185°K, we find that the conduction is largely intrinsic but analysis is complicated by the fact that the energy gap and Fermi energy are the same order of magnitude. The precise values of E_g and dE_g/dT are thus critical. The relevant statistics under these and other circumstances are discussed by Verié.[18] A plot of N versus T is shown in Fig. 14. These N values were determined from 70-GHz helicon interferometry. We find that $N \propto T^s$ with s slowly increasing from 1.5 to 2 as the temperature is increased from 77 to 185°K. It is possible to describe this variation and to estimate the effective mass of the holes, m_h^*, by assuming that the concentration of ionized donors, n_{di}, is relatively small and constant, or slowly varying. Using Eqs. (1), (4), and (9) with the experimental values of $N(T)$, we computed the Fermi energy ϕ in

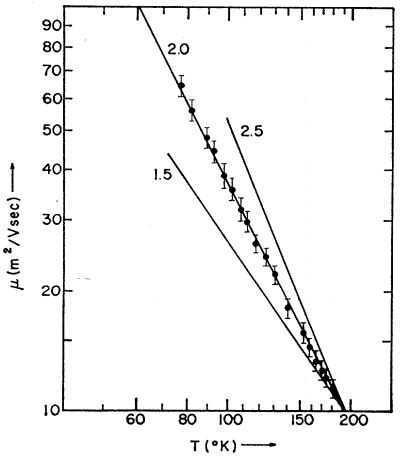

FIG. 13. Plot of $\ln\mu$ versus $\ln T$ using μ values obtained from amplitude analysis of the data taken for sample I at 24 GHz. The lines are drawn with slopes of −1.5, −2.0, and −2.5.

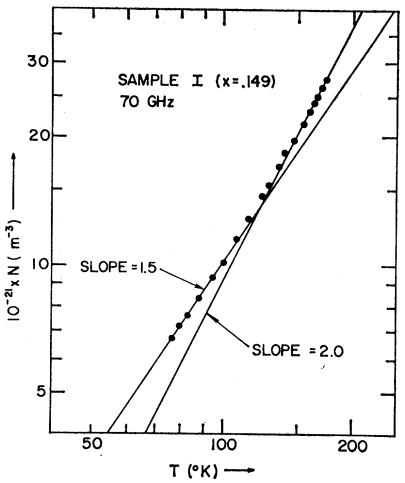

FIG. 14. Plot of $\ln N$ versus $\ln T$ using data taken for sample I at 24 GHz. It is found that $N \propto T^s$, with s increasing from 1.5 to 2.0 as shown here.

the conduction band. Then,[36] because classical statistics is appropriate for the valence band,

$$N(T)=4.83\times10^{21}(m_h^*/m_0)^{3/2}T^{3/2}e^{-(E_g+\phi)/kT}+n_{di}, \quad (15)$$

where n_{di} is the concentration of ionized donors, and we have arbitrarily assumed that the valence band is parabolic and spherical. Only m_h^* and n_{di} are unknown in this equation. If n_{di} is assumed to be constant from 77 to 185°K, it is possible to estimate m_h^*. (The carrier concentration at 1.3°K, 2×10^{21} m^{-3}, probably represents a lower limit of n_{di} for all temperatures, but it is not necessary to assume this.) Actually, due to the change in energy gap, electronic effective mass, and Fermi energy with temperature, n_{di} is unlikely to be constant. Nevertheless, the observed $N(T)$ is well described by Eq. (15), as shown in Fig. 15 for a partic-

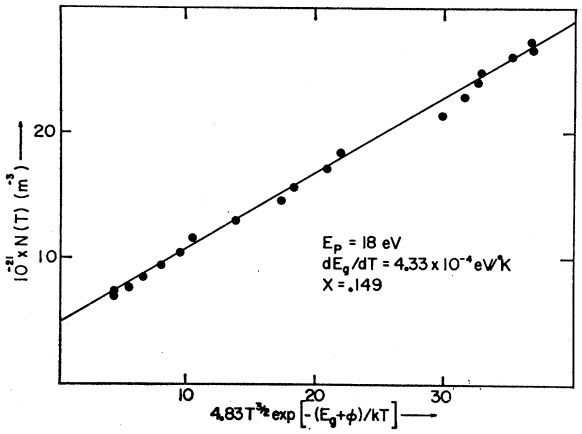

FIG. 15. Experimental values of $N(T)$ plotted according to Eq. (15) for particular parameters and assuming n_{di} is constant. The slope of the straight line is $(m_h^*/m_0)^{3/2}$ and the intercept gives n_{di}. For this figure $m_h^*=0.715m_0$ and $n_{di}=4.5\times10^{21}$ m^{-3}.

[36] J. S. Blakemore, *Semiconductor Statistics* (Pergamon Press, Inc., New York, 1962).

ular choice of dE_g/dT, E_P, and the recorded x value. Similar calculations and plots of comparable quality were made for a significant range of variation of these empirical parameters. The slope of the straight line plotted in the manner of Fig. 15 is equal to $(m_h^*/m_0)^{3/2}$. The resulting estimate of m_h^* is $(0.71\pm0.05)m_0$, where the quoted error includes the variation of m_h^* measured from the slopes of such lines with $0.147\leq x\leq 0.151$, $E_P=18$ or 19 eV, and $dE_g/dT=4.33\times10^{-4}$ eV/°K or 5.0×10^{-4} eV/°K for HgTe. It is unlikely that the parameters are outside of these ranges but the assumptions of the model are in more serious question; our assumption of a parabolic and spherical valence band is an oversimplification,[37,38] and n_{di} may not be constant over the temperature range 77–185°K. Depending on the assumed parameters, we calculated $4.0\times10^{21}\leq n_{di}\leq5.4\times10^{21}$ m^{-3} with the above assumptions. Our estimate of m_h^* is in accord with other estimates for HgTe[37] and $Hg_{0.9}Cd_{0.1}$ Te[38] based on thermoelectric power measurements. We conclude that the accepted band model is quite satisfactory for describing our observations; there exist heavy holes with $m_h^*\gg m_e^*$ and the variation of N with temperature is dominated by the preexponential $T^{3/2}$ in Eq. (15).

IV. SUMMARY

We have used microwave helicons and nonresonant cyclotron absorption to measure N, μ, and m^* for seven samples of $Hg_{1-x}Cd_xTe$ with $0.135\leq x\leq0.203$. The carrier concentrations were sufficiently low to enable us to measure m^* values closer to the conduction-band edge than usually reported for samples in this x range. We find that the measured m^* values at 77 and 1.3°K are in good agreement with the predictions of Kane's model for the conduction band. No systematic deviations were observed. Consequently, we are unable to suggest values for E_g, dE_g/dT, or P which are improved over numbers found in the literature. The free-carrier contribution to the dielectric constant was considerably larger than the lattice contribution and hence prevented accurate determinations of ϵ_L.

A study was made of the temperature dependence of N, μ, and m^* for one sample ($x=0.149$) at 1.3°K and from 77 to 185°K. From this study we obtained additional confirmation of the applicability of Kane's model and our assumed expression for $E_g(x,T)$. We were also able to obtain an estimate of 0.71 ± 0.05 for the hole effective mass. The mobility was found to be proportional to T^{-2} between 77 and 185°K, but the data were too limited to justify extensive analysis or speculation concerning scattering mechanisms.

ACKNOWLEDGMENTS

We would like to thank Dr. J. Schmit, Dr. D. Long, and Dr. D. Zook of the Honeywell Corporate Research Center for their generosity in providing us with samples and for several useful discussions during the course of this work. We are also grateful to Dr. A. J. Strauss of the Lincoln Laboratory, MIT, for additional samples.

[37] I. I. Ivanov-Omskii, F. P. Kesamanly, B. T. Kolomiets, A. Sh. Mekhtiev, and V. A. Shripkin, Phys. Status Solidi **27**, K169 (1968).

[38] R. R. Galazka and T. Zakrewski, Phys. Status Solidi **23**, K39 (1967).